ERDC/CRREL TR-22-2

Cold Regions Research
and Engineering Laboratory

US Army Corps
of Engineers®
Engineer Research and
Development Center

ERDC
ENGINEER RESEARCH & DEVELOPMENT CENTER

Terrain Conditions Forecasting

Implementation of an Albedo-Based Drag Partition into the WRF-Chem v4.1 AFWA Dust Emission Module

Michelle L. Michaels, Theodore W. Letcher, Sandra L. LeGrand,
Nicholas P. Webb, and Justin B. Putnam

January 2022

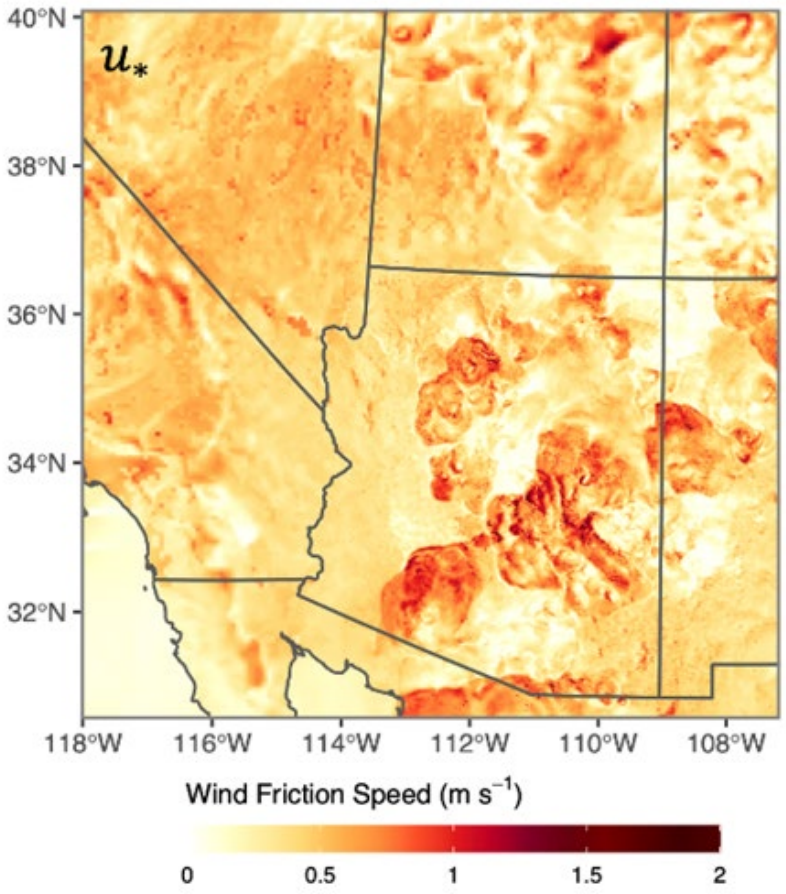

The U.S. Army Engineer Research and Development Center (ERDC) solves the nation's toughest engineering and environmental challenges. ERDC develops innovative solutions in civil and military engineering, geospatial sciences, water resources, and environmental sciences for the Army, the Department of Defense, civilian agencies, and our nation's public good. Find out more at www.erdc.usace.army.mil.

To search for other technical reports published by ERDC, visit the ERDC online library at https://erdclibrary.on.worldcat.org/discovery.

ERDC/CRREL TR-22-2
January 2022

Implementation of an Albedo-Based Drag Partition into the WRF-Chem v4.1 AFWA Dust Emission Module

Michelle L. Michaels, Theodore W. Letcher, Sandra L. LeGrand, and Justin B. Putnam

U.S. Army Engineer Research and Development Center (ERDC)
Cold Regions Research and Engineering Laboratory (CRREL)
72 Lyme Road
Hanover, NH 03755-1290

Nicholas P. Webb

U.S. Department of Agriculture–Agricultural Research Service
Jornada Experimental Range
MSC 3 JER, New Mexico State University, Box 30003
Las Cruces, NM 88003

Final Report

Prepared for Headquarters, US Army Corps of Engineers
Washington, DC 20314-1000

Under PE 0603463A, Project BP4, Task SBP402, Terrain Conditions Forecasting,
"ERDC-Geo Dust Source Characterization: Advanced Capability Demonstration"

Abstract

Employing numerical prediction models can be a powerful tool for forecasting air quality and visibility hazards related to dust events. However, these numerical models are sensitive to surface conditions. Roughness features (e.g., rocks, vegetation, furrows, etc.) that shelter or attenuate wind flow over the soil surface affect the magnitude and spatial distribution of dust emission. To aide in simulating the emission phase of dust transport, we used a previously published albedo-based drag partition parameterization to better represent the component of wind friction speed affecting the immediate soil surface. This report serves as a guide for integrating this parameterization into the Weather Research and Forecasting with Chemistry (WRF-Chem) model. We include the procedure for preprocessing the required input data, as well as the code modifications for the Air Force Weather Agency (AFWA) dust emission module. In addition, we provide an example demonstration of output data from a simulation of a dust event that occurred in the Southwestern United States, which incorporates use of the drag partition.

Contents

Figures and Tables

Figures

Tables

Preface

This study was conducted for Headquarters, U.S. Army Corps of Engineers, under PE 0603463A, Project BP4, Task SBP402, Terrain Conditions Forecasting, "ERDC-Geo Dust Source Characterization: Advanced Capability Demonstration."

The work was performed by the Force Projection and Sustainment Branch (Dr. Wade Lein, acting chief) and the Terrestrial and Cryospheric Sciences Branch (Dr. John Weatherly, chief) of the Research and Engineering Division, U.S. Army Engineer Research and Development Center, Cold Regions Research and Engineering Laboratory (ERDC-CRREL). At the time of publication, Dr. George Calfas was division chief. The deputy director of ERDC-CRREL was Mr. David B. Ringelberg, and the director was Dr. Joseph L. Corriveau.

COL Teresa A. Schlosser was commander of ERDC, and Dr. David W. Pittman was the director.

1 Introduction

1.1 Background

It is vital that numerical forecasting models can robustly and accurately predict and simulate dust emission events. Dust storms greatly affect human health, agriculture, mobility, equipment performance, water supply, and infrastructure (e.g., De Longueville et al. 2010; Okin et al. 2011; Sprigg et al. 2014; Clow et al. 2016; Al-Hemoud et al. 2017; Middleton 2017; Schweitzer et al. 2018; Bhattachan et al. 2019; Rushingabigwi et al. 2020). Also, dust storms degrade visibility, which can double as tactical advantage opportunities for battlespace concealment. Accurate dust emission representations are critical for modeling the overall lifecycle and transport of airborne dust (Muhs et al. 2014). Therefore, improved dust emission characterizations are essential to U.S. Army operations and mission planning for dryland regions.

Drag partitioning occurs where roughness elements, such as rocks and vegetation, create aerodynamic drag and influence wind flow over the ground. The remaining wind shear stress at the soil surface influences the amount and spatial patterns of sediment transport (Webb et al. 2020) and should be represented in dust entrainment models for effective dust emission characterization.

1.2 Objectives

Researchers at the U.S. Army Engineer Research and Development Center (ERDC) are currently exploring techniques for incorporating drag partition theory into existing dust emission models for research and operational planning applications. This report documents procedures for implementing an albedo-based drag partition parameterization by Chappell and Webb (2016) into a dust emission module within the Weather Research and Forecasting model with Chemistry (WRF-Chem).

Our objectives are as follows:

- To document the procedure for preparing the required input data

- To demonstrate how to implement the Chappell and Webb (2016) parameterization into the Air Force Weather Agency (AFWA) dust emission module
- To provide an example of how the drag partition affects the model output

1.3 Approach

We assembled this report primarily as a user's guide and organized as follows: Section 2 provides an overview of the albedo-based drag partition parameterization and the required input datasets. In section 3, we describe the AFWA module and how the drag partition affects the equations governing dust emission. Section 4 offers instructions on how to implement the drag partition into the WRF-Chem v4.1 AFWA module code. In section 5, we provide a qualitative demonstration of how the drag partition implementation affects a simulated convective dust event. Forthcoming publications will present more in-depth model evaluations.

2 Drag Partition Parameterization

2.1 Overview

In dust emission modeling, wind friction speed (u_*, m s^{-1})[2] is an important scalar physical parameter used to represent the wind shear stress acting on the terrain surface. Furthermore, u_* can be partitioned such that

$$u_* = u_{r*} + u_{s*}, \quad (1)$$

where u_{r*} is the component of u_* that is acting directly on roughness elements and u_{s*} is the component acting on the immediate soil surface. Effectively, the u_{s*} component governs the dust emission process rather than the overall u_*.

Chappell and Webb (2016) established a method using measured albedo to parameterize u_{s*} in dust emission models. Essentially, their technique assumes shadows cast by roughness elements can serve as a proxy for the sheltered-area extent (Figure 1). As described in Ziegler et al. (2020),

$$u_{s*} = U_{10m} \times u_{ns*}, \quad (2)$$

where U_{10m} is the wind speed 10 m above ground level and u_{ns*} is a daily normalized u_{s*} parameter (unitless) derived from albedo.

Figure 1. Example of a surface-roughness element casting a shadow, which we can leverage to calculate the sheltered-area extent. The presence of a roughness element can attenuate the wind flow and produce a sheltered-terrain surface area.

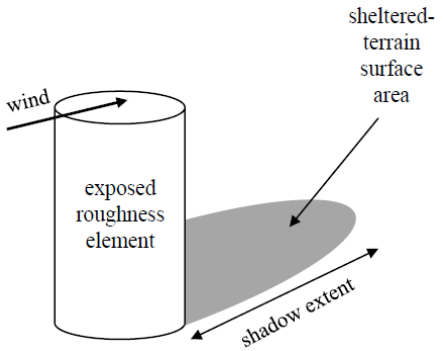

[2] For a full list of the spelled-out forms of the units of measure used in this document, please refer to *U.S. Government Publishing Office Style Manual*, 31st ed. (Washington, DC: U.S Government Publishing Office, 2016), 248–252, https://www.govinfo.gov/content/pkg/GPO-STYLEMANUAL-2016/pdf/GPO-STYLEMANUAL-2016.pdf.

2.2 u_{ns*} determined from albedo data

To quantify areal estimates of u_{ns*} for use in WRF-Chem, we calculated surface shadowing from the 500 m Moderate Resolution Imaging Spectroradiometer (MODIS) Bidirectional Reflectance Distribution Function (BRDF) albedo product: Collection 6, MCD43A1 (Schaaf and Wang 2015). Following Chappell and Webb (2016) and Ziegler et al. (2020), we determined the normalized proportion of shadow, ω_n, via

$$\omega_n = \frac{1-\omega_{dir}(0°)}{f_{iso}}, \quad (3)$$

where $\omega_{dir}(0°)$ is the daily nadir "black-sky" albedo for MODIS band 1 (620–670 nm wavelength) and f_{iso} is a BRDF isotropic weighting parameter, included in the MCD43A1 dataset. Here, "black-sky" albedo (directional hemispherical reflectance) refers to albedo in the absence of a diffuse component and is a function of solar zenith angle (Schaaf and Wang 2015). We then calculated daily u_{ns*}:

$$u_{ns*} = 0.0311\left(exp\frac{-{\omega_{ns}}^{1.131}}{0.016}\right) + 0.007, \quad (4)$$

where ω_{ns} represents an empirically scaled proportion of shadow obtained by

$$\omega_{ns} = \frac{(a-b)(\omega_n-35)}{-35} + b, \quad (5)$$

where a = 0.0001 and b = 0.1.

3 Dust Emission Model

3.1 WRF-Chem overview

The WRF model is a nonhydrostatic, atmospheric modeling system (Skamarock et al. 2019). WRF-Chem is a specialized version of WRF that incorporates atmospheric transport, mixing, and feedback processes of gases and aerosols (Grell et al. 2005; Fast et al. 2006). Designed to be highly configurable, WRF-Chem includes several built-in submodels that users can choose to activate depending on their application of interest and computational resources. For this demonstration, we added the Chappell and Webb (2016) drag partition to the AFWA dust emission module (LeGrand et al. 2019) in WRF-Chem version 4.1 (Werner 2019) and ran simulations with the Georgia Institute of Technology–Goddard Global Ozone Chemistry Aerosol Radiation and Transport (GOCART) model (Chin et al. 2000; Ginoux et al. 2001) option in WRF-Chem. Though we used WRF-Chem v4.1 in this implementation example, the process should be relatively consistent with later model versions (on version 4.3 at the time of publication). Note, we recommend that readers planning to use WRF-Chem/GOCART work with version 4.1 or later due to a critical bug fix in the GOCART deposition module.

3.2 Overview of the AFWA dust emission module

The AFWA dust emission module (LeGrand et al. 2019) is an adaptation of the dust emission scheme initially described by Marticorena and Bergametti (1995). In the AFWA code, wind-driven dust entrainment occurs through a process called *saltation*, where wind-lofted particles too heavy to remain suspended in the airstream collide with the land surface and dislodge smaller "dust-sized" particles (~0.1–20 μm) on impact (e.g., Bagnold 1941; Kok et al. 2012). The AFWA module equations, which are in terms of u_*, include the static threshold friction speed necessary for particle mobilization (u_{*t}), the horizontal saltation flux (Q), and the bulk vertical dust flux (F_B). Once known, F_B converts to a size-resolved emitted dust flux using a prescribed particle-size distribution curve so the GOCART model can disperse size-resolved dust aerosol concentrations.

Simulated saltation processes initiate and cease as u_* values exceed or fall below u_{*t}, respectively. First, the module establishes u_{*t} (cm s^{-1}) estimates for air-dry soil conditions based on saltation-particle diameter ($D_{s,p}$). The

code then applies a correction for soil moisture, *f(θ)*, based on the method developed by Fécan et al. (1999) to adjust the mobilization thresholds for the effects of soil moisture on particle cohesion:

$$u_{*t,s,p} = u_{*t}(D_{s,p}) f(\theta). \tag{6}$$

Here, $D_{s,p}$ represents a preset array of nine saltation-particle sizes ranging from 1.42 μm (clay-sized particles) to 250 μm (fine sand). Next, the module determines size-resolved saltation-flux ($Q_{s,p}$) estimates for each particle size in the prescribed $D_{s,p}$ array:

$$Q_{s,p} = \begin{cases} C \frac{\rho_a}{g} {u_*}^3 \left(1 + \frac{u_{*t,s,p}}{u_*}\right)\left(1 - \frac{{u_{*t,s,p}}^2}{{u_*}^2}\right), & u_* > u_{*t,s,p}, \\ 0, & u_* \le u_{*t,s,p} \end{cases} \tag{7}$$

where

C = a constant set to 1.0,
ρ_a = atmospheric density, and
g = the acceleration due to gravity.

The code then obtains the total streamwise horizontal saltation flux, Q (g cm^{-1} s^{-1}), for each model grid cell by summing $Q_{s,p}$ values weighted by the surficial soil composition fraction associated with each saltation-particle size at a given grid location.

After calculating Q, the module translates the horizontal saltation flux into the bulk vertical dust emission flux (F_B; g cm^{-2} s^{-1}) by multiplying Q by a topographic-based, dust-source strength parameter (S) and a sandblasting efficiency factor (β) inferred from the soil clay fraction. The F_B function also includes a conditional statement based on aerodynamic roughness length (z_0) to limit dust emission to regions with relatively sparse vegetation coverage:

$$F_B = \begin{cases} Q\beta S, & z_0 \le 20 \text{ cm} \\ 0, & z_0 > 20 \text{ cm} \end{cases}. \tag{8}$$

The z_0 parameter represents the theoretical height above the land surface where the mean wind speed becomes zero under neutral (i.e., stable) atmospheric conditions. In general, the presence of roughness elements in-

creases the z_0 value for a given location though the structure and configuration of the individual roughness elements will vary the effect (e.g., Mayaud and Webb 2017). For example, the z_0 of a densely forested area will likely be higher than the z_0 of a grassland. Often, numerical weather models, including WRF-Chem, assume z_0 conditions based on prescribed land-use designations. The 20 cm threshold assumed for equation (8) generally restricts dust emission from urban and forested areas, but the extent of the z_0 conditional's effect will ultimately depend on how the model user configures their land surface attribute settings.

The S parameter represents the availability of loose, erodible soil material that accumulates in topographic basins based on the surface elevation surrounding a model grid cell (Ginoux et al. 2001):

$$S = \left(\frac{z_{\max} - z_i}{z_{\max} - z_{\min}}\right)^5, \tag{9}$$

where z_i is the model grid cell elevation and $z_{\max}$ and $z_{\min}$ are the maximum and minimum elevation in the surrounding 10° × 10° area, respectively. Essentially, this approach assumes that erodible material accumulates in terrain depressions.

Although domain-relative elevation values are available within WRF-Chem, the AFWA module incorporates S from a precalculated 1/4° resolution field interpolated to the model domain. This built-in S parameter also includes a static vegetation mask that restricts dust emission from locations designated as vegetated. However, because this static vegetation mask was computed from an annual average land cover dataset derived from 1° resolution Advanced Very High Resolution Radiometer (AVHRR) 1987 data, it does not represent temporal variability in vegetation.

3.3 Drag partition incorporation

To incorporate the Chappell and Webb (2016) drag partition into AFWA dust emission equations, we replaced u_* values in the $Q_{s,p}$ calculation (equation 7) with u_{s*} estimates from equation (2):

$$Q_{s,p} = \begin{cases} C\frac{\rho_a}{g}{u_{s*}}^3\left(1 + \frac{u_{*t,s,p}}{u_{s*}}\right)\left(1 - \frac{{u_{*t,s,p}}^2}{{u_{s*}}^2}\right), & u_{s*} > u_{*t,s,p} \\ 0, & u_{s*} \le u_{*t,s,p} \end{cases}. \tag{10}$$

Furthermore, we removed any lingering parameters from the original AFWA equations that functioned as stopgaps for vegetation or roughness effects. Specifically, we eliminated the z_0 conditional threshold and the S parameter from equation (8):

$$F_B = Q\beta. \tag{11}$$

The z_0 dependency removal is relatively straightforward since it primarily serves as a vegetation mask. However, omitting the S parameter also removes the available sediment supply component of equation (8). From a modeling perspective, this forces the AFWA module to treat all locations as preferential dust sources (i.e., S = 1). Replacing the built-in WRF-Chem S field without the 1987 AVHRR vegetation mask, though, is beyond the scope of this effort.

4 Implementation of the Drag Partition in WRF-Chem

This section offers step-by-step instructions for implementing the Chappell and Webb (2016) drag partition into the AFWA dust emission module in WRF-Chem v4.1. Here, we cover how to

1. procure and preprocess MODIS-derived u_{ns^*} data,
2. modify the model run-time configuration file,
3. update the model variable registry, and
4. incorporate all necessary code changes to the AFWA dust emission module.

Note, the code blocks provided in this section show only the modified code components. Full modules with all modifications included for WRF-Chem v4.1 are publicly accessible at Michaels (2021).

4.1 Overview

Figure 2 provides a schematic overview of the WRF-Chem model structure for directories and files discussed in this report. This example layout assumes all model source code and executables reside in a top-level directory called "WRF-4.1 Parent Directory." Figure 2 shows within this parent directory two subdirectories containing the WRF Preprocessing System (WPS) and the main model source code ("WPS-4.1" and "WRF-4.1", respectively). WPS executables prepare the environmental forcing datasets that drive the model. All of the code modifications presented in this report occur in the main model source code directory. The naming scheme and architecture adopted here for these three particular directories is somewhat arbitrary, assuming the user sets their directory paths properly when configuring and compiling their own model source code. However, the directories and files from the lowest directory level in Figure 2 should be consistent across all model implementations.

Although the MODIS-derived u_{ns^*} data required by the drag partition qualify as environmental forcing data, our implementation procedure ingests u_{ns^*} data directly through an auxiliary input channel as the model runs (rather than through WPS). Section 4.2 describes the method we used for acquiring and preprocessing u_{ns^*} data. Model users, however, are free to develop their own approaches if the resultant input dataset follows the same formatting.

Figure 2. WRF-Chem model architecture with respect to directories and files referenced in this report. Directories are in *boxes*, and files are in *italics*.

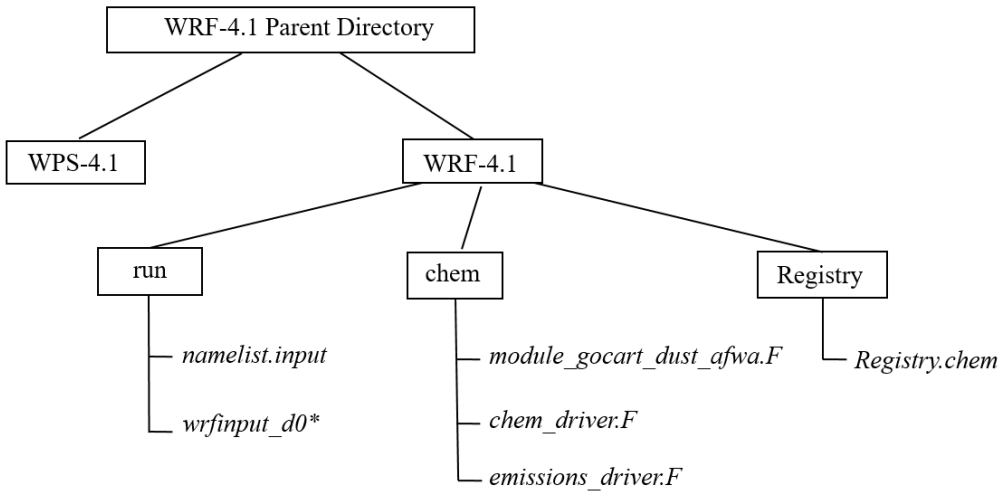

Sections 4.3 and 4.4 provide detailed source code and configuration file modification procedures designed so users can easily switch back and forth between the original and modified model versions without having to recompile their code. To better enable simulation sensitivity testing, we added four new run-time configuration settings to the code (see Table 1). The default model setting (labeled in this report as OPT0) activates the original AFWA dust emission code without the Chappell and Webb (2016) drag partition. The first alternate setting (OPT1) replaces the u_* values feeding into the AFWA dust emission equations with u_{s*} (i.e., equation 10). The last two configuration setting options (OPT2 and OPT3) also incorporate u_{s*} but remove the influence of other roughness or vegetation related parameters from the bulk dust emission flux calculation. Both the OPT2 and OPT3 configurations eliminate the z_0 conditional from equation (8) while only the OPT3 option sets the S parameter equal to 1 (i.e., OPT3 uses equations 10 and 11). Importantly, this coding approach enables model developers to systematically test the drag partition's influence on simulation outcomes. In general, removing the vegetation masks and replacing u_* with u_{s*} in equation (7) makes the AFWA dust emission module more consistent with our current understanding of aeolian transport physics.

Table 1. Model run-time configuration options.

Label	Size-Resolved Saltation Equation	Bulk Dust Flux Equation
OPT0	$Q_{s,p} = \begin{cases} C\frac{\rho_a}{g}{u_*}^3\left(1+\frac{u_{*t,s,p}}{u_*}\right)\left(1-\frac{{u_{*t,s,p}}^2}{{u_*}^2}\right), & u_* > u_{*t,s,p} \\ 0, & u_* \le u_{*t,s,p} \end{cases}$	$F_B = \begin{cases} QS\beta, & z_0 \le 20\text{cm} \\ 0, & z_0 > 20\text{cm} \end{cases}$
OPT1	$Q_{s,p} = \begin{cases} C\frac{\rho_a}{g}{u_{s*}}^3\left(1+\frac{u_{*t,s,p}}{u_{s*}}\right)\left(1-\frac{{u_{*t,s,p}}^2}{{u_{s*}}^2}\right), & u_{s*} > u_{*t,s,p} \\ 0, & u_{s*} \le u_{*t,s,p} \end{cases}$	$F_B = \begin{cases} QS\beta, & z_0 \le 20\text{cm} \\ 0, & z_0 > 20\text{cm} \end{cases}$
OPT2	$Q_{s,p} = \begin{cases} C\frac{\rho_a}{g}{u_{s*}}^3\left(1+\frac{u_{*t,s,p}}{u_{s*}}\right)\left(1-\frac{{u_{*t,s,p}}^2}{{u_{s*}}^2}\right), & u_{s*} > u_{*t,s,p} \\ 0, & u_{s*} \le u_{*t,s,p} \end{cases}$	$F_B = QS\beta$
OPT3	$Q_{s,p} = \begin{cases} C\frac{\rho_a}{g}{u_{s*}}^3\left(1+\frac{u_{*t,s,p}}{u_{s*}}\right)\left(1-\frac{{u_{*t,s,p}}^2}{{u_{s*}}^2}\right), & u_{s*} > u_{*t,s,p} \\ 0, & u_{s*} \le u_{*t,s,p} \end{cases}$	$F_B = Q\beta$

4.2 u_{ns*} data preprocessing requirements

4.2.1 MODIS BRDF data acquisition and u_{ns*} calculation

We suggest using Google Earth Engine (https://earthengine.google.com/) to obtain u_{ns*} data. A user can import the necessary input data to Google Earth Engine by calling the 500 m MODIS BRDF product Earth Engine image collection (referenced in Google Earth Engine as MCD43A1) and selecting both the band 1 (620–670 nm) black-sky albedo and the band 1 isotropic parameter for a specific period and location of interest. These two datasets equate to $\omega_{dir}(0°)$ and the f_{iso} parameter from equation (3), respectively. Note, the band 1 isotropic parameter must be rescaled by a factor of 0.001. By using the Google Earth Engine scripting platform, developers can diagnose u_{ns*} with these two datasets and the calculation procedure described in section 2.2 (equations 3–5). The user can then export the resultant u_{ns*} data in GeoTIFF format.

4.2.2 u_{ns*} data preprocessing for WRF-Chem

Before we can use the MODIS-derived values from section 4.2.1, we must first align the u_{ns*} data to the WRF-Chem grid domain and convert the data to a Network Common Data Form (NetCDF) file format using a separate, stand-alone Python script called ModisUSTtoWRFInput.py (provided in Appendix A). NetCDF is a standard format for sharing array-oriented scientific data (see UCAR 2021). The georeferencing functions in

ModisUSTtoWRFInput.py leverage domain information from a WRF input file with the naming convention "wrfinput_d01" (in this case, *d01* refers to *domain 1*). Note, the "wrfinput_d0*" files are output by the "real.exe" executable, which users run as a first step in the simulation process when using the actual WRF-Chem model (a step that comes after the WPS stage is complete).

As seen in Figure 2 above, the model stores the "wrfinput_d0*" files in the "run" subfolder of the main WRF-Chem source code directory. Note, the script provided in Appendix A assumes the WRF-Chem model uses a Lambert conformal conic map projection. Users interested in applying other WRF projection options, such as Mercator or the global latitude-longitude setting, must update the script accordingly.

4.3 Namelist file modifications

Generally, simulation models require a run-time configuration file. These configuration files usually include settings for domain information, date and time, run-time interval, grid nesting, map projection, etc. In the case of WRF and other specialized WRF versions like WRF-Chem, we call these configuration files *namelists*. For example, "namelist.wps" and "namelist.input" are the run-time configuration files for WPS and the main WRF model, respectively. For further documentation of the "namelist.input" file options specific to WRF-Chem, please see Earth System Research Laboratory (n.d.).

The WRF model can support nested model domains to downscale environmental conditions to finer resolutions. In a namelist, any particular parameter can store multiple columns of data associated with it. The namelist parameter called `max_dom` sets the number of domains to be modeled. For example, if `max_dom` is set to 2 and there are three columns of data, only the first two columns will be ingested into the model. Any given parameter that has multiple columns of data for multiple nests is considered domain relative. Conversely, a parameter with only one possible column of data is a global setting.

Here, we cover modifications to the "namelist.input" file for activating the albedo-based drag partition in a dust model simulation. Note, these are only the file modifications and not the full "namelist.input" file. We refer readers to Appendix B for a complete "namelist.input" file example. There are no modifications to the "namelist.wps" file to document.

4.3.1 New "namelist.input" file parameters

In the "namelist.input" file, we add a variable termed `modis_dust_ust` to the chem (`&chem`) section to activate one of the four options described in section 4.1. For example, the following code block would configure the AFWA dust emission module by setting `dust_opt = 3`. To run with OPT3 activated, we set `modis_dust_ust = 3`:

```
&chem
kemit                = 1,
.
.
.
dust_opt             = 3,
modis_dust_ust       = 3,
.
.
.

/
```

The new `modis_dust_ust` variable has a few required conditions associated for it to work properly and not cause model run-time issues. For example, the maximum possible value it should be set to is 3. As stated above, this corresponds to OPT3. If `modis_dust_ust` is set to a value higher than 3, it will automatically default to a value of 3 and run that configuration option. In addition, this parameter should be set to an integer value only. If `modis_dust_ust` is not set to any value in the "namelist.input" file, this parameter will automatically default to a value of 0, which corresponds to the original model configuration (OPT0, no drag partition included). Additionally, the model will run into a critical error if the `modis_dust_ust` parameter is included in the "namelist.input" file prior to compiling the source code modifications. In the next subsection, we cover the auxiliary input channel requirements, which are additional parameters added to the "namelist.input" file. Section 4.4.2 provides a deeper description of the model implications behind the `modis_dust_ust` variable.

4.3.2 Settings to read u_{ns*} data through an auxiliary channel

If the user opts to activate the drag partition (i.e., `modis_dust_ust` = 1, 2, or 3), the "namelist.input" file will also need to include information on how to

read and interpret the user-provided u_{ns^*} input file described in section 4.2. To set up the auxiliary input channel, a user must add the optional parameters `auxinput12_inname`, `auxinput12_interval`, and `io_form_auxinput12` to the end of the namelist `&time_control` section. Note that the number "12" in these parameter names indicates that the model will ingest the u_{ns^*} data through auxiliary channel number 12. We chose channel 12 specifically because WRF-Chem v4.1 already had (mostly undocumented) built-in data-feed designations associated with several of the other auxiliary channels. If readers using later version of WRF-Chem encounter errors with channel 12, trial and error or searching the source code for explicit channel calls may be necessary to find an open auxiliary channel.

The `auxinput12_inname` parameter should be set to a file with the prefix "wrf_ust_input_d<domain>", where <domain> is a 2-digit integer (including leading zeros), which corresponds to the grid nest identification number. The channel 12 auxiliary input filename can include multiple wrf_ust_input files, corresponding to each nested domain.

In the following namelist example, the model will expect to find a file named "wrf_ust_input_d<domain>" for domains 1, 2, and 3. Furthermore, we set the interval value to 100,000 minutes for each nested domain since this corresponds to an arbitrarily long simulation that ensures we treat the input roughness data as a static field over the course of the simulation.

The `io_form_auxinput` parameter indicates the file format. In this case, we are expecting the file to be in NetCDF format, indicated by the number "2."

In the example below, we show a "namelist.input" file with a triple nested grid as shown by the association of each domain-relative parameter with three columns of values.

```
&time_control
run_days            = 0,
run_hours           = 48,
run_minutes         = 0,
run_seconds         = 0,
start_year          = 2014, 2014, 2014,
start_month         = 07, 07, 07,
.
.
```

```
.
auxinput12_inname   = "wrf_ust_input_d01", "wrf_ust_in-
put_d02", "wrf_ust_input_d03",
auxinput12_interval = 100000,100000,100000,
io_form_auxinput12  = 2,
/
```

4.4 Source code modifications

Once the model ingests the preprocessed u_{ns*} values, WRF-Chem stores them within the main grid data structure. This arrangement effectively means there is no need to add any new code for passing u_{ns*} data through the model architecture. As illustrated in Figure 3, the main chemistry driver ("chem_driver.F") reads the entire grid structure. While running, the chemistry driver initiates the emissions driver ("emissions_driver.F"), which passes the u_{ns*} data to the AFWA dust emission module ("module_gocart_dust_afwa.F"). The only required source code modifications occur in the model variable registry and the AFWA dust emission module. Importantly, these modifications affect only the AFWA dust emission code. They do not apply to the other physics packages in the WRF-Chem framework that use u_*.

Figure 3. Normalized friction speed data flow within WRF-Chem.

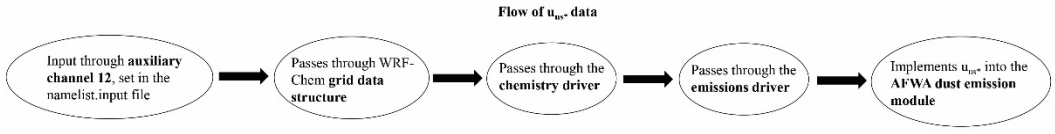

4.4.1 Updating the WRF registry

The purpose of the WRF registry file is to easily add namelist variables without the need for extensively editing model source code. To implement the drag partition, we added three new variables to the "registry.chem" file, located in the "Registry" subfolder of the main WRF-4.1 source code directory (see Figure 2). These variables include `norm_ust` (u_{ns*} in symbol form), `ust_soil_only` (the wind friction speed value used by the AFWA module to drive the dust emission equations), and `modis_dust_ust` (the new drag partition activation namelist parameter described in section 4.3.1). Following the required format structure for WRF-Chem v4.1, we modified the "registry.chem" file by adding:

```
state real norm_ust ij misc 1 - i{12}rh02
"NORM_UST" "MODIS normalized Ust values for dust emission
potential" "none"

state real ust_soil_only ij misc 1  - h02
"UST_SOIL_ONLY" "Modified Ust value for dust emission po-
tential scaled by MODIS normalized Ust values (NORM_UST)"
"m s^-1"

rconfig integer modis_dust_ust namelist,chem  1 0 rh
"modis_dust_ust" "" ""
```

Note, setting `modis_dust_ust` greater than or equal to 1 instructs the dust transport model to use the modified `ust_soil_only` value. If `modis_dust_ust` = 0, then the model does not apply this modified variable and runs in its original configuration. Section 4.4.2 explains this in more detail.

4.4.2 AFWA dust emission code modifications

We made the following code changes to "module_gocart_dust_afwa.F", located in the "chem" directory (Figure 2). Note, the text provided here only highlights our code modifications. Please see https://github.com/MichelleLMichaels/WRF-Chem-v4.1-AFWA-Dust-Module-Modifications.git for a complete version of the modified "module_gocart_dust_afwa.F" code.

As discussed previously, the new `modis_dust_ust` "namelist.input" file parameter informs the AFWA module how to set the wind friction speed driving the dust emission equations (`ustar` in the AFWA module code) such that

$$\text{ustar} = \begin{cases} u_{ns*}\sqrt{u_{10m}^2 + v_{10m}^2}, & \text{modis\_dust\_ust} \geq 1 \\ u_*, & \text{modis\_dust\_ust} = 0 \end{cases}, \tag{12}$$

where u_{10m} and v_{10m} correspond to the zonal (east–west) and meridional (north–south) components, respectively, of the wind velocity 10 m above ground level. Note, the top portion of equation (12) is identical to equation (2) for u_{s*} but written in terms of wind speed components. Depending on the `modis_dust_ust` parameter setting, `ustar` will be equal to either u_* or u_{s*}.

The following block shows equation (12) in code form:

```
if(config_flags%modis_dust_ust .ge. 1) then
   localust(i,j)=ust(i,j)*(u10(i,j)**2+v10(i,j)**2)**0.5
   ust_soil_only(i,j)=localust(i,j)
endif
if(config_flags%modis_dust_ust .ge. 1) then
     ustar(1,1)=localust(i,j)
  else
     ustar(1,1)=ustar(1,1)
  endif
```

Here, `i` and `j` are domain grid indices, `ust` is the MODIS-derived u_{ns^*} input read in through the auxiliary channel, and `u10` and `v10` are the model-diagnosed zonal and meridional components, respectively, of wind speed 10 m above ground level. The code holds the resultant u_{s^*} values in two arrays called `localust` and `ust_soil_only`. The `localust` array is a temporary array used to pass u_{s^*} values in the AFWA code while the `ust_soil_only` array feeds the resultant u_{s^*} values to the simulation output file. If `modis_dust_ust` greater than or equal to 1, the module uses the u_{s^*} values stored in `localust` to set `ustar`. Otherwise, `ustar` remains unaffected (i.e., `ustar` = u_*).

The next module code modification includes a conditional statement to check if `modis_dust_ust` is greater than or equal to 3. If so, then S (`erodtot` in the code) is set to a value of 1.0 everywhere:

```
IF(config_flags%modis_dust_ust .ge. 3) then
         erodtot(1,1)=1.0
```

Lastly, we incorporate code to remove the z_0 mask. At locations with `modis_dust_ust` less than 2, the code applies a mask at grid points with z_0 greater than 0.2 m. If `modis_dust_ust` greater than or equal to 2, the module ignores the adjustment. As a reminder, the default model configuration includes the z_0 mask.

```
   IF(config_flags%modis_dust_ust .lt. 2) then
      IF (znt(i,j) .gt. 0.2) then
         ilwi(1,1)=0
      ENDIF
   ENDIF
```

Here, `znt` is the time-varying, model-provided z_0 value; and `ilwi` is a binary parameter used to mask nonerodible areas in the vertical dust emission flux equation.

5 Demonstration

In this section, we provide a qualitative demonstration of how the implementation of the drag partition into the AFWA module affects the simulation of a convective dust event from 3–4 July 2014 that affected the city of Phoenix, Arizona (33.45 °N, 112.067 °W), in the southwestern United States. Figure 4 shows the three telescoping model domains for our dust event simulation (D01, D02, and D03, hereafter) with grid resolutions of 18 km, 6 km, and 2 km, respectively. We produced four simulations, including one for each of the AFWA dust emission module configuration options described in Table 1. The configuration settings used for these simulations given by the "namelist.input" and "namelist.wps" files are included in Appendices B and C, respectively.

Figure 4. WRF-Chem nested model domains with terrain elevation in meters.

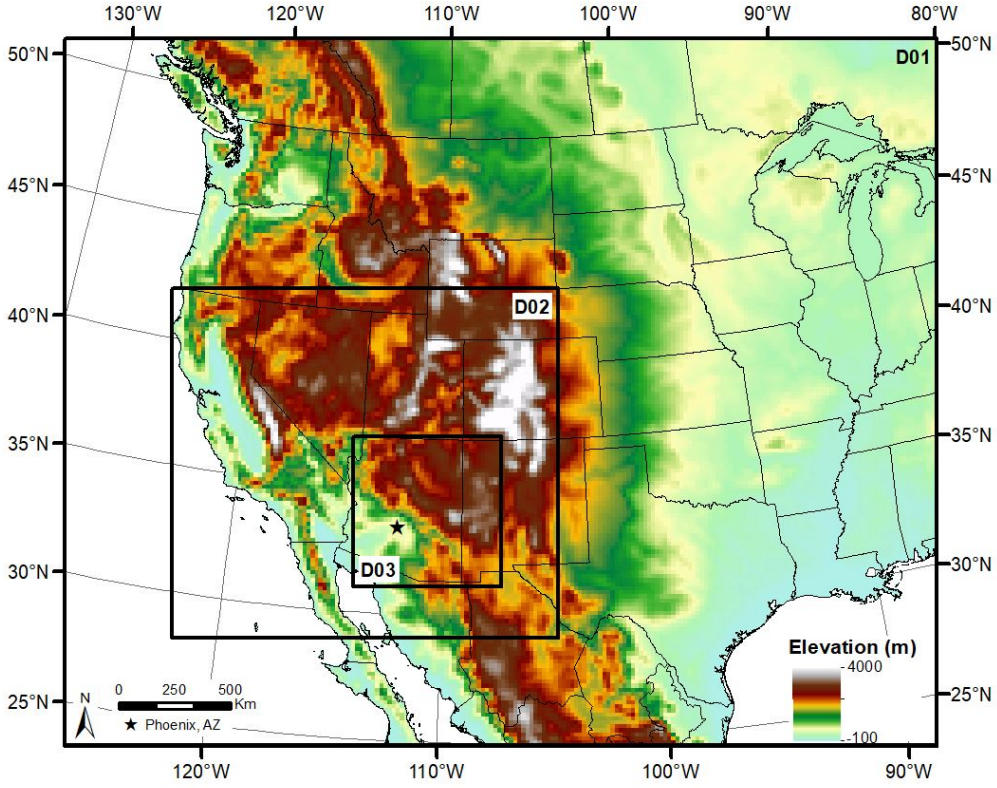

During the convective dust event, a wall of dust crossed over the Phoenix metropolitan area between 0000 and 0400 UTC on 4 July 2014. Importantly, once the main dust wall passed, the air quality conditions rapidly recovered, and the areas outside of the immediate dust event were relatively clear. According to surface weather station records (not pictured),

it is unlikely the dust obscurations extended much beyond the Phoenix metropolitan area.

Figure 5 delineates areas around our region of interest above and below the 20 cm z_0 threshold. For our example model configuration settings, the z_0 mask restricts dust emission to areas prescribed as grasslands, barren or sparsely vegetated areas, cropland, and open shrublands in the in OPT0 and OPT1 simulations. In Arizona, this blocks the terrain from emitting dust in the forested mountain zones and built-up urban areas around Phoenix.

Figure 5. Aerodynamic roughness length mask for D02 and D03.

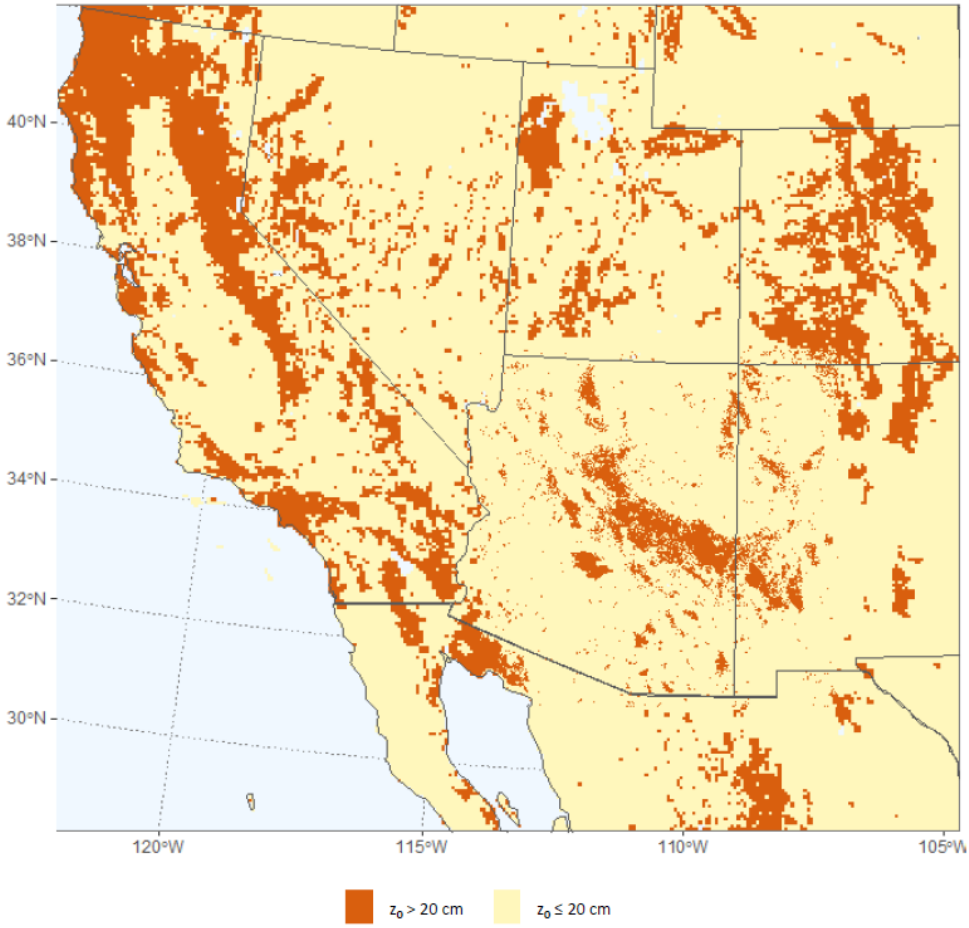

As referenced in section 2.1, u_{s*} is the component of the wind friction speed (u_*) that acts on the immediate soil surface. In Figure 6, we exemplify the output differences between overall u_* and the u_{s*} component for our simulations with the drag partition parameterization applied. The friction speed values at the immediate land surface reduced by approximately

a factor of four. The area around Phoenix is primarily classified as open shrublands according to the MODIS International Geosphere-Biosphere Programme land cover classification system. In the original AFWA module configuration (OPT0), the model behaves as if the landscape were completely smooth and barren in the area where the dust event occurred. It is clear that implementing the Chappell and Webb (2016) drag partition provides a means to capture the local vegetation effects without having to completely restrict dust emissions in the presence of vegetation.

Figure 6. Simulated u_* (*left*) and u_{s*} (*right*) fields associated with the peak of the dust event on 4 July 2014 at 0200 UTC.

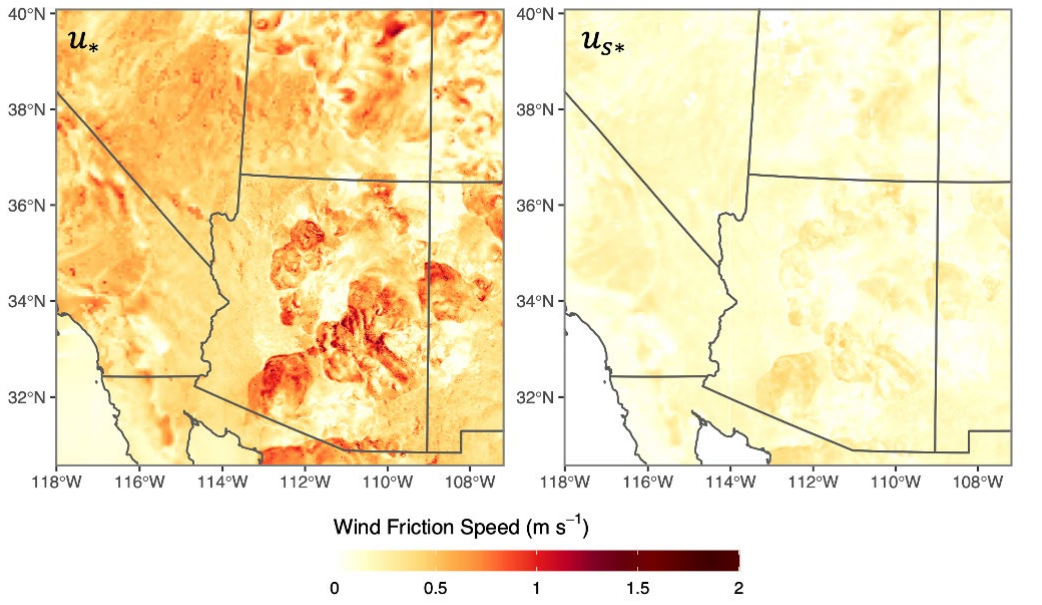

Because the area where the storm took place is in a terrain lowland with z_0 primarily less than 20 cm conditions and no prescribed vegetation coverage in the *S* field, minor simulation differences between the spatial patterns of dust parameters associated with OPT1, OPT2, and OPT3 were relatively negligible. There were no discernable differences in simulated magnitude between the OPT1 and OPT2 outcomes, while results from the OPT3 simulation were higher magnitude and more aligned with observed conditions recorded by nearby Environmental Protection Agency stations that monitor concentrations of particulate matter up to 10 μm in diameter (PM10). For example, the near-surface PM10 fields simulated by OPT3 were approximately 2000 to 5000 μg m^{-3} higher than the PM10 fields produced by the OPT1 and OPT2 simulations near the storm outflow boundary. However, this increase in magnitude of dust parameters from OPT3

over OPT1 and OPT2 was relatively consistent across all locations that produced dust, meaning the *S* parameter from equations (8) and (9) behaved like a relatively constant global tuning parameter in the areas where dust emission occurred. Accordingly, we chose to focus on simulation results from OPT0 and OPT3 to exemplify the influence of the drag partition.

As expected, the original AFWA configuration (OPT0) captured a strong dust signal along the convective outflow boundary (Figure 7), but it also generated widespread dust concentrations in areas that, in reality, were clear. The magnitude and spatial pattern of the simulated PM10 values associated with the OPT3 configuration aligned better with reported observations (not pictured). The new drag partition treatment suppressed the extensive plume in southern California and southwestern Arizona as compared to the control without restricting dust emissions that generated the Phoenix dust storm.

Figure 7. Simulated PM10 concentrations associated with the peak of the dust event on 4 July 2014 at 0200 UTC, generated using the OPT0 (*left*) and OPT3 (*right*) model configurations.

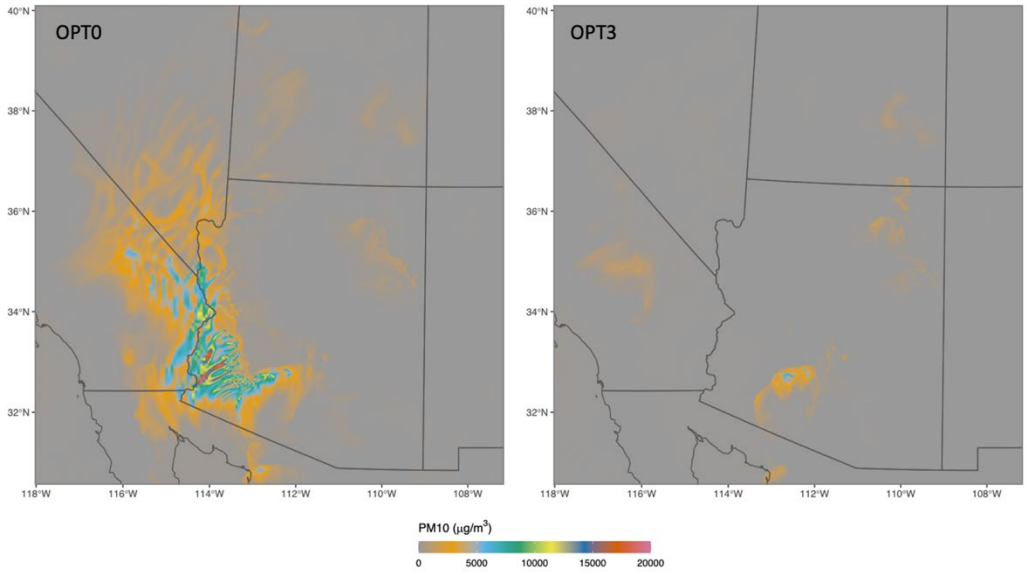

6 Conclusions

In this report, we demonstrated and provided instructions for how to implement into a dust emission model an albedo-based drag partition parameterization developed by Chappell and Webb (2016). We described how to prepare the required input datasets and to set up the AFWA dust emission module to run model simulations with the new drag partition treatment in WRF-Chem. We also demonstrated a test example over the southwestern United States of model output generated using the new drag partition parameterization.

As demonstrated, incorporating the drag partition parameterization can improve model-simulated dust emission results. Without this parameterization, modeled results may overestimate dust production in areas with low-density vegetation or overrestrict dust from emitting in vegetated drylands. This is an important consideration when applying modeled dust results to operational visibility forecasting capabilities.

While the MODIS-derived u_{ns*} field varies over time, the WRF-Chem implementation procedure described in this report treats u_{ns*} as a static (time invariant) field. We suspect that this approach is appropriate for a majority of daily weather forecasting applications since the roughness elements typically do not change on the characteristic timescale for individual dust storms (i.e., hours to days). Future efforts could expand this capability to be time variable for seasonal or climate applications, including transient changes in dust emissions due to plant phenology patterns, drought, land management practices, or land cover change.

Though this report focuses on integration specifically with the WRF-Chem model, readers should be able to apply a similar method to other physics-based dust emission models. Validation case studies headed by ERDC are currently underway to assess simulation efforts of a dust events in dryland regions. These case studies will include further use and testing of the parameterization covered in this report.

References

Al-Hemoud, A., M. Al-Sudairawi, S. Neelamanai, A. Naseeb, and W. Behbehani. 2017. "Socioeconomic Effect of Dust Storms in Kuwait." *Arabian Journal of Geosciences* 10 (1): 18. https://doi.org/10.1007/s12517-016-2816-9.

Bagnold, R. A. 1941. *The Physics of Blown Sand and Desert Dunes*. London: Methuen.

Bhattachan, A., G. S. Okin, J. Zhang, S. Vimal, and D. P. Lettenmaier. 2019. Characterizing the Role of Wind and Dust in Traffic Accidents in California. *GeoHealth* 3 (10): 328–336. https://doi.org/10.1029/2019GH000212.

Chappell, A., and N. P. Webb. 2016. "Using Albedo to Reform Wind Erosion Modelling, Mapping and Monitoring." *Aeolian Research* 23 (December):63–78. https://doi.org/10.1016/j.aeolia.2016.09.006.

Chin, M., D. L. Savoie, B. J. Huebert, A. R. Bandy, D. C. Thornton, T. S. Bates, P. K. Quinn, E. S. Saltzman, and W. J. De Bruyn. 2000. "Atmospheric Sulfur Cycle Simulated in the Global Model GOCART: Comparison with Field Observations and Regional Budgets." *Journal of Geophysical Research: Atmospheres* 105 (D20): 24689–24712. https://doi.org/10.1029/2000JD900385.

Clow, D. W., M. W. Williams, and P. F. Schuster. 2016. "Increasing Aeolian Dust Deposition to Snowpacks in the Rocky Mountains Inferred from Snowpack, Wet Deposition, and Aerosol Chemistry." *Atmospheric Environment* 146 (December):183–194. https://doi.org/10.1016/j.atmosenv.2016.06.076.

De Longueville, F., Y.-C. Hountondji, S. Henry, and P. Ozer. 2010. What Do We Know about Effects of Desert Dust on Air Quality and Human Health in West Africa Compared to Other Regions?" *Science of The Total Environment* 409 (1): 1–8. https://doi.org/10.1016/j.scitotenv.2010.09.025.

Earth System Research Laboratory. n.d. "WRF namelist.input File Description." Earth System Research Laboratory, Global Systems Division. Accessed 2 November 2021. https://esrl.noaa.gov/gsd/wrfportal/namelist_input_options.html.

Fast, J. D., W. I. Gustafson Jr., R. C. Easter, R. A. Zaveri, J. C. Barnard, E. G. Chapman, G. A. Grell, and S. E. Peckham. 2006. "Evolution of Ozone, Particulates, and Aerosol Direct Forcing in an Urban Area Using a New Fully-Coupled Meteorology, Chemistry, and Aerosol Model." *Journal of Geophysical Research* 111 (D21): D21305. https://doi.org/10.1029/2005JD006721.

Fécan, F., B. Marticorena, and G. Bergametti. 1999. "Parametrization of the Increase of the Aeolian Erosion Threshold Wind Friction Velocity Due to Soil Moisture for Arid and Semi-Arid Areas." *Annales Geophysicae* 17 (1): 149–157.

Ginoux, P., M. Chin, I. Tegen, J. M. Prospero, B. Holben, O. Dubovik, and S.-J. Lin. 2001. "Sources and Distributions of Dust Aerosols Simulated with the GOCART Model." *Journal of Geophysical Research* 106 (D17): 20255–20273. https://doi.org/10.1029/2000JD000053.

Grell, G. A., S. E. Peckham, R. Schmitz, S. A. McKeen, G. Frost, W. C. Skamarock, and B. Eder. 2005. "Fully Coupled 'Online' Chemistry within the WRF Model." *Atmospheric Environment* 39 (37): 6957–6975. https://doi.org/10.1016/j.atmosenv.2005.04.027.

Kok, J. F., E. J. R. Parteli, T. I. Michaels, and D. Bou Karam. 2012. "The Physics of Wind-Blown Sand and Dust." *Reports on Progress in Physics* 75 (10): 106901. https://doi.org/10.1088/0034-4885/75/10/106901.

LeGrand, S. L., C. Polashenski, T. W. Letcher, G. A. Creighton, S. E. Peckham, and J. D. Cetola. 2019. The AFWA Dust Emission Scheme for the GOCART Aerosol Model in WRF-Chem v3.8.1. *Geoscientific Model Development* 12 (1): 131–166. https://doi.org/10.5194/gmd-12-131-2019.

Marticorena, B., and G. Bergametti. 1995. "Modeling the Atmospheric Dust Cycle: 1. Design of a Soil-Derived Dust Emission Scheme." *Journal of Geophysical Research* 100 (D8): 16415. https://doi.org/10.1029/95JD00690.

Mayaud, J. R., and N. P. Webb 2017. "Vegetation in Drylands: Effects on Wind Flow and Aeolian Sediment Transport." *Land* 6 (3): 64. https://doi.org/10.3390/land6030064.

Michaels, M. L. 2021. *WRF-Chem-v4.1-AFWA-Dust-Module-Modifications*. Hanover, NH: U.S. Army Engineer Research and Development Center, Cold Regions Research and Engineering Laboratory. https://github.com/MichelleLMichaels/WRF-Chem-v4.1-AFWA-Dust-Module-Modifications.

Middleton, N. J. 2017. "Desert Dust Hazards: A Global Review." *Aeolian Research* 24 (February): 53–63. https://doi.org/10.1016/j.aeolia.2016.12.001.

Muhs, D. R., J. M. Prospero, M. C. Baddock, and T. E. Gill. 2014. "Identifying Sources of Aeolian Mineral Dust: Present and Past." In *Mineral Dust: A Key Player in the Earth System*, edited by Peter Knippertz and Jan-Berend W. Stuut, 51–74. Dordrecht: Springer Netherlands. https://doi.org/10.1007/978-94-017-8978-3_3.

Okin, G. S., J. E. Bullard, R. L. Reynolds, J.-A. C. Ballantine, K. Schepanski, M. C. Todd, J. Belnap, M. C. Baddock, T. E. Gill, and M. E. Miller. 2011. "Dust: Small-Scale Processes with Global Consequences." *Eos, Transactions American Geophysical Union* 92 (29): 241–242. https://doi.org/10.1029/2011EO290001.

Rushingabigwi, G., P. Nsengiyumva, L. Sibomana, C. Twizere, and W. Kalisa. 2020. "Analysis of the Atmospheric Dust in Africa: The Breathable Dust's Fine Particulate Matter PM2.5 in Correlation with Carbon Monoxide." *Atmospheric Environment* 224 (March): 117319. https://doi.org/10.1016/j.atmosenv.2020.117319.

Schaaf, C., and Z. Wang. 2015. *MCD43A1 MODIS/Terra+Aqua BRDF/Albedo Model Parameters Daily L3 Global - 500m V006*. Distributed by NASA EOSDIS Land Processes DAAC. Accessed 22 September 2021. https://doi.org/10.5067/MODIS/MCD43A1.006.

Schweitzer, M. D., A. S. Calzadilla, O. Salamo, A. Sharifi, N. Kumar, G. Holt, M. Campos, and M. Mirsaeidi. 2018. "Lung Health in Era of Climate Change and Dust Storms." *Environmental Research* 163 (May): 36–42. https://doi.org/10.1016/j.envres.2018.02.001.

Skamarock., W. C., J. B. Klemp, J. Dudhia, D. O. Gill, Z. Liu, J. Berner, W. Wang, J. G. Powers, M. G. Duda, D. M. Barker, and X.-Y. Huang. 2019. *A Description of the Advanced Research WRF Version 4*. NCAR/TN–556+STR. Boulder, Colorado: National Center for Atmospheric Research, Mesoscale and Microscale Meteorology Division.

Sprigg, W. A., S. Nickovic, J. N. Galgiani, G. Pejanovic, S. Petkovic, M. Vujadinovic, A. Vukovic, M. Dacic, S. DiBiase, A. Prasad, and H. El-Askary. 2014. "Regional Dust Storm Modeling for Health Services: The Case of Valley Fever." *Aeolian Research* 14 (September): 53–73. https://doi.org/10.1016/j.aeolia.2014.03.001.

UCAR. 2021. "Network Common Data Form (NetCDF)." Unidata. https://www.unidata.ucar.edu/software/netcdf/.

Webb, N. P., A. Chappell, S. L. LeGrand, N. P. Ziegler, and B. L. Edwards. 2020. "A Note on the Use of Drag Partition in Aeolian Transport Models." *Aeolian Research* 42 (January): 100560. https://doi.org/10.1016/j.aeolia.2019.100560.

Werner, K. 2019. *WRF Version 4.1*. Boulder, CO: National Center for Atmospheric Research. https://github.com/wrf-model/WRF/releases/tag/v4.1.

Ziegler, N. P., N. P. Webb, A. Chappell, and S. L. LeGrand. 2020. "Scale Invariance of Albedo-Based Wind Friction Velocity." *Journal of Geophysical Research: Atmospheres* 125 (16): e2019JD031978. https://doi.org/10.1029/2019JD031978.

Appendix A: ModisUSTtoWRFInput.py

This section includes the ModisUSTtoWRFInput.py script referenced in section 4.2.2. In the following code, there are a few user-defined parameters that must be set before use. They are as follows:

geopath: the directory path set to the location of the landcover data files

wrfpath: the directory path set to the location of the main WRF source code directory

wrf_input_path: the directory path set to the location of the "wrfinput.do<domain>" files

nests: the number of grid nests applied to the specific simulation run

Additionally, the user must set the `geotiff_proj` parameter in the code to the proper map projection based on the specific input GeoTIFF files.

```
from osgeo import gdal
from cartopy import crs as ccrs
from cartopy import feature as cfeature
from scipy.interpolate import griddata
from matplotlib import pyplot as plt
import glob as glob
import numpy as np
from netCDF4 import Dataset
gdal.UseExceptions()

geopath='/.../.../'
wrfpath='/.../.../'
wrf_input_path='/.../.../'

wrfout_name='NORM_UST'
nests=['…']


plt.figure(figsize=(16,12))
ax=plt.subplot(111,projection=ccrs.PlateCarree())
for ndx, n in enumerate(nests):
```

```
geotiff_file=glob.glob(geopath+'*d0%s*.tif'%n)[0]
wrfoutfile=glob.glob(wrfpath+'*%s*.nc'%n)[0]

wrf_ustfile=glob.glob(wrf_input_path+'*d0%s'%n)[0]

geoglobe=ccrs.Globe()
gtif = gdal.Open(geotiff_file)
gt=gtif.GetGeoTransform()
proj=gtif.GetProjection()

# The following map projection is to be set by the user
based on their input geo files #
geotiff_proj=ccrs.LambertConformal(central_latitude=39.0000
04,central_longitude=-
108,standard_parallels=[39,39],globe=geoglobe)

geodata=np.flipud(gtif.ReadAsArray())
x=np.arange(gt[0],gt[0]+gt[1]*geodata.shape[1],gt[1])
y=np.arange(gt[3],gt[3]+gt[5]*geodata.shape[0],gt[5])
y=y[::-1]
gtif.close()

x,y=np.meshgrid(x,y)

geodata=np.ma.masked_less(geodata,0.00001).filled(0.00001)

wrf_data=Dataset(wrfoutfile,'r')
lon=wrf_data.variables['XLONG'][0,:].squeeze()
lat=wrf_data.variables['XLAT'][0,:].squeeze()
vari=wrf_data.variables['LANDMASK'][0,:].squeeze()

cent_lon=wrf_data.STAND_LON
cent_lat=wrf_data.MOAD_CEN_LAT
std_pars=[wrf_data.TRUELAT1,wrf_data.TRUELAT2]

proj_data=[cent_lat,cent_lon]+std_pars

wrf_data.close()
```

```
proj=ccrs.LambertConformal(central_longitude=proj_data[1],
central_latitude=proj_data[0],

      false_easting=0.0, false_northing=0.0,
      secant_latitudes=None,
      standard_parallels=proj_data[2:], globe=None)

inproj=ccrs.PlateCarree()
transform=geotiff_proj.transform_points(inproj,
np.array(lon), np.array(lat))

xx=transform[:,:,0]
yy=transform[:,:,1]

xx_z2 = griddata((x.ravel(),y.ravel()), x.ravel(), (xx,
yy), method='linear')
yy_z2 =  griddata((x.ravel(),y.ravel()), y.ravel(), (xx,
yy), method='linear')
rough_z2 = griddata((x.ravel(),y.ravel()), geodata.ravel(),
(xx, yy), method='linear')

rough_z2=np.ma.masked_invalid(rough_z2).filled(0.00001)
transform=inproj.transform_points(geotiff_proj,
np.array(xx_z2), np.array(yy_z2))
lon_z2=transform[:,:,0]
lat_z2=transform[:,:,1]

Z=ax.contourf(lon,lat,np.ma.masked_less(rough_z2,0.00001),c
map='coolwarm',levels=np.linspace(0.0,0.035,41))

## NOW OUTPUT TO DATA! ##
datafile=wrf_input_path + 'wrf_ust_input_d0%s'%n
infile=glob.glob(wrf_input_path + 'wrfinput_d0%s'%n)[0]

vname='TSK'
print(datafile)
src=Dataset(infile,'r')
dst=Dataset(datafile, "w",format='NETCDF3_CLASSIC')
# copy global attributes all at once via dictionary
dst.setncatts(src.__dict__)
```

```
# copy dimensions
for name, dimension in src.dimensions.items():
      dst.createDimension(
            name, (len(dimension) if not
            dimension.isunlimited() else None))

for nn, variable in src.variables.items():
      if nn == vname:
            print("DOING DATA!")
            x = dst.createVariable(wrfout_name,np.float32,
            variable.dimensions)
            dst[wrfout_name][0,:] = rough_z2[:]
            # copy variable attributes all at once via
            dictionary
            dst[wrfout_name].setncatts(src[vname].__dict__)
            dst[wrfout_name].description='MODIS Normalized
            ustar'
            dst[wrfout_name].units='-'
            break

times=src.variables['Times']
print(times)
print(np.shape(times))

x=dst.createVariable('Times','S1', times.dimensions)
dst['Times'][:]=times[:]

src.close()
dst.close()
print("DONE!")
```

Appendix B: Namelist.input File Used for Implementation Testing

```
&time_control
 run_days                            = 1,
 run_hours                           = 18,
 run_minutes                         = 0,
 run_seconds                         = 0,
 start_year                          = 2014, 2014, 2014,
 start_month                         = 07, 07, 07,
 start_day                           = 03, 03, 03,
 start_hour                          = 00, 00, 00,
 start_minute                        = 00, 00, 00,
 start_second                        = 00, 00, 00,
 end_year                            = 2014, 2014, 2014,
 end_month                           = 07, 07, 07,
 end_day                             = 04, 04, 04,
 end_hour                            = 18, 18, 18,
 end_minute                          = 00, 00, 00,
 end_second                          = 00, 00, 00,
 interval_seconds                    = 10800,
 input_from_file                     = .true.,.true.,.true.,
 history_interval                    = 60,60,30,
 frames_per_outfile                  = 1, 1, 1,
 restart                             = .false.,
 restart_interval                    = 180,
 io_form_history                     = 2,
 io_form_restart                     = 2,
 io_form_input                       = 2,
 io_form_boundary                    = 2,
 debug_level                         = 5,
 auxinput1_inname                    = "met_em.d<domain>.<date>",
 force_use_old_data                  = .true.,

 auxinput5_inname                    = 'wrfchemi_d<domain>',
 auxinput8_inname                    = 'wrfchemi_gocart_bg_d<domain>',
 io_form_auxinput5 = 2,
 io_form_auxinput8 = 2,
 auxinput5_interval_m = 100000,100000,100000,
 auxinput8_interval_m = 100000,100000,100000,

 auxinput12_inname = "wrf_ust_input_d<domain>",
```

```
 auxinput12_interval = 100000,100000,100000,
 io_form_auxinput12 = 2,

/

 &domains
 time_step                           = 90,
 time_step_fract_num                 = 0,
 time_step_fract_den                 = 1,
 max_dom                             = 3,
 s_we                                =   1,   1,   1,
 e_we                                = 223, 286, 340,
 s_sn                                =   1,   1,   1,
 e_sn                                = 176, 262, 340,
 e_vert                              = 41, 41, 41,
 num_metgrid_levels                  = 40,
 num_metgrid_soil_levels             = 4,
 dx                                  = 18000, 6000, 2000,
 dy                                  = 18000, 6000, 2000,
 grid_id                             = 1, 2, 3,
 parent_id                           = 0, 1, 2,
 i_parent_start                      = 1, 35, 135,
 j_parent_start                      = 1, 27, 40,
 parent_grid_ratio                   = 1, 3, 3,
 parent_time_step_ratio              = 1, 3, 3,
 p_top_requested                     = 5000,
 feedback                            = 0,
 smooth_option                       = 0,
 zap_close_levels                    = 50,
 interp_type                         = 2,
 t_extrap_type                       = 2,
 force_sfc_in_vinterp                = 0,
 use_levels_below_ground             = .true.,
 use_surface                         = .true.,
 lagrange_order                      = 1,
 /
 sfcp_to_sfcp                        = .true.,
&physics
 num_land_cat                        = 21,
 mp_physics                          = 8, 8, 8,
 progn                               = 0,
 ra_lw_physics                       = 4, 4, 4,
 ra_sw_physics                       = 4, 4, 4,
```

```
radt                                = 5,
sf_sfclay_physics                   = 5, 5, 5,
sf_surface_physics                  = 2, 2, 2,
bl_pbl_physics                      = 5, 5, 5,
bldt                                = 0,
cu_physics                          = 14, 14, 0,
cu_diag                             = 1,
cudt                                = 0,
ishallow                            = 0,
isfflx                              = 1,
ifsnow                              = 1,
icloud                              = 1,
icloud_bl                           = 1,
surface_input_source                = 1,
num_soil_layers                     = 4,
sf_urban_physics                    = 0,
mp_zero_out                         = 0,
maxiens                             = 1,
maxens                              = 3,
maxens2                             = 3,
maxens3                             = 16,
ensdim                              = 144,
slope_rad                           = 1,
topo_shading                        = 0,
cu_rad_feedback                     = .true.,
do_radar_ref                        = 1,
/


&fdda
/

&dynamics
rk_ord                              = 3,
w_damping                           = 1,
diff_opt                            = 1,
km_opt                              = 4,
diff_6th_opt                        = 0,    0,    0,
diff_6th_factor                     = 0.12, 0.12, 0.12,
damp_opt                            = 1,
zdamp                               = 5000.,
dampcoef                            = 0.02, 0.02, 0.02,
khdif                               = 0,  0,  0,
```

```
kvdif                               = 0,  0,  0,
non_hydrostatic                     = .true., .true., .true.,
moist_adv_opt                       = 1,
scalar_adv_opt                      = 1,
chem_adv_opt                        = 1,
tke_adv_opt                         = 1,
time_step_sound                     = 4,
h_mom_adv_order                     = 5,
v_mom_adv_order                     = 3,
h_sca_adv_order                     = 5,
v_sca_adv_order                     = 3,
/

&bdy_control
spec_bdy_width                      = 5,
spec_zone                           = 1,
relax_zone                          = 4,
specified                           = .true., .false., .false.,
nested                              = .false., .true., .true.,
/

&grib2
/

&chem
kemit                               = 1,
chem_opt                            = 301, 301, 301,
bioemdt                             = 0,
photdt                              = 0,
chemdt                              = 0,
io_style_emissions                  = 2,
modis_dust_ust                      = 3,
emiss_opt                           = 5,          5, 5,
emiss_inpt_opt                      = 1,
emiss_opt_vol                       = 0,          0, 0,
emiss_ash_hgt                       = 20000.,
chem_in_opt                         = 0,          0, 0,
phot_opt                            = 0,          0, 0,
gas_drydep_opt                      = 1,          1, 1,
aer_drydep_opt                      = 1,          1, 1,
bio_emiss_opt                       = 0,          0, 0,
ne_area                             = 0,
dust_opt                            = 3,
```

```
 dust_schme                          = 3,
 dmsemis_opt                         = 1,
 seas_opt                            = 1,
 depo_fact                           = 0.25,
 gas_bc_opt                          = 1,          0, 0,
 gas_ic_opt                          = 1,          0, 0,
 aer_bc_opt                          = 1,          0, 0,
 aer_ic_opt                          = 1,          0, 0,
 gaschem_onoff                       = 0,          0, 0,
 aerchem_onoff                       = 0,          0, 0,
 wetscav_onoff                       = 0,          0, 0,
 cldchem_onoff                       = 0,          0, 0,
 vertmix_onoff                       = 0,          0, 0,
 chem_conv_tr                        = 0,          0, 0,
 conv_tr_wetscav                     = 0,          0, 0,
 conv_tr_aqchem                      = 0,          0, 0,
 biomass_burn_opt                    = 0,          0, 0,
 plumerisefire_frq                   = 30,         0, 0,
 have_bcs_chem                       = .false., .false., .false.,
 aer_ra_feedback                     = 0,
 aer_op_opt                          = 2,          2, 2,
 opt_pars_out                        = 1,
 diagnostic_chem                     = 0,
/

 &namelist_quilt
 nio_tasks_per_group = 0,
 nio_groups = 1,
 /
```

Appendix C: Namelist.wps File Used for Implementation Testing

```
&share
 wrf_core = 'ARW',
 max_dom = 3,
 start_date = '2014-07-03_00:00:00', '2014-07-03_00:00:00',
'2014-07-03_00:00:00',
 end_date   = '2014-07-04_18:00:00', '2014-07-04_18:00:00',
'2014-07-04_18:00:00',
 interval_seconds = 10800
 io_form_geogrid = 2,
 debug_level = 0
/

&geogrid
 parent_id         =   1,   1,   2,
 parent_grid_ratio =   1,   3,   3,
 i_parent_start    =   1,  35,  135,
 j_parent_start    =   1,  27,  40,
 e_we              =  223, 286, 340,
 e_sn              =  176, 262, 340,
 !
 !!!!!!!!!!!!!!!!!!!!!!!!!! IMPORTANT NOTE
!!!!!!!!!!!!!!!!!!!!!!!!!!
 ! The default datasets used to produce the MAXSNOALB and
ALBEDO12M
 ! fields have changed in WPS v4.0. These fields are now
interpolated
 ! from MODIS-based datasets.
 !
 ! To match the output given by the default namelist.wps in WPS
v3.9.1,
 ! the following setting for geog_data_res may be used:
 !
 ! geog_data_res = 'maxsnowalb_ncep+albedo_ncep+default',
'maxsnowalb_ncep+albedo_ncep+default',
 !
```

```
 !!!!!!!!!!!!!!!!!!!!!!!!!! IMPORTANT NOTE
!!!!!!!!!!!!!!!!!!!!!!!!!!!
 !
 geog_data_res = 'default','default','default'
 dx = 18000,
 dy = 18000,
 map_proj = 'lambert',
 ref_lat   =  39.00,
 ref_lon   =  -108.00,
 truelat1  =  39.0,
 truelat2  =  39.0,
 stand_lon =  -108.00,
 geog_data_path = '/'
/

&ungrib
 out_format = 'WPS',
 prefix = '',
/

&metgrid
 fg_name = '',
 io_form_metgrid = 2,
/
```

Acronyms and Abbreviations

AFWA	Air Force Weather Agency
AVHRR	Advanced Very High Resolution Radiometer
BRDF	Bidirectional Reflectance Distribution Function
CRREL	Cold Regions Research and Engineering Laboratory
ERDC	U.S. Army Engineer Research and Development Center
GOCART	Global Ozone Chemistry Aerosol Radiation and Transport
MODIS	Moderate Resolution Imaging Spectroradiometer
NetCDF	Network Common Data Form
OPT0	Control Dust Module Configuration
OPT1	Alternate Option Module Configuration 1
OPT2	Alternate Option Module Configuration 2
OPT3	Alternate Option Module Configuration 3
PM10	Particulate Matter up to 10 μm in Diameter
WPS	WRF Preprocessing System
WRF	Weather Research and Forecasting
WRF-Chem	Weather Research and Forecasting with Chemistry

REPORT DOCUMENTATION PAGE

Form Approved
OMB No. 0704-0188

1. REPORT DATE (DD-MM-YYYY)	2. REPORT TYPE	3. DATES COVERED (From - To)
January 2022	Technical Report / Final	FY20–FY21

4. TITLE AND SUBTITLE
Implementation of an Albedo-Based Drag Partition into the WRF-Chem v4.1 AFWA Dust Emission Module

5a. CONTRACT NUMBER

5b. GRANT NUMBER

5c. PROGRAM ELEMENT
0603463A

6. AUTHOR(S)
Michelle L. Michaels, Theodore W. Letcher, Sandra L. LeGrand, Nicholas P. Webb, and Justin B. Putnam

5d. PROJECT NUMBER
BP4

5e. TASK NUMBER
SBP402

5f. WORK UNIT NUMBER

7. PERFORMING ORGANIZATION NAME(S) AND ADDRESS(ES)

U.S. Army Engineer Research and Development Center (ERDC)
Cold Regions Research and Engineering Laboratory (CRREL)
72 Lyme Road
Hanover, NH 03755-1290

U.S. Department of Agriculture–Agricultural Research Service
Jornada Experimental Range
MSC 3 JER, New Mexico State University, Box 30003
Las Cruces, NM 88003

8. PERFORMING ORGANIZATION REPORT NUMBER
ERDC/CRREL TR-22-2

9. SPONSORING / MONITORING AGENCY NAME(S) AND ADDRESS(ES)
Headquarters, US Army Corps of Engineers
Washington, DC 20314-1000

10. SPONSOR/MONITOR'S ACRONYM(S)
USACE

11. SPONSOR/MONITOR'S REPORT NUMBER(S)

12. DISTRIBUTION / AVAILABILITY STATEMENT
Approved for public release; distribution is unlimited.

13. SUPPLEMENTARY NOTES

14. ABSTRACT

Employing numerical prediction models can be a powerful tool for forecasting air quality and visibility hazards related to dust events. However, these numerical models are sensitive to surface conditions. Roughness features (e.g., rocks, vegetation, furrows, etc.) that shelter or attenuate wind flow over the soil surface affect the magnitude and spatial distribution of dust emission. To aide in simulating the emission phase of dust transport, we used a previously published albedo-based drag partition parameterization to better represent the component of wind friction speed affecting the immediate soil surface. This report serves as a guide for integrating this parameterization into the Weather Research and Forecasting with Chemistry (WRF-Chem) model. We include the procedure for preprocessing the required input data, as well as the code modifications for the Air Force Weather Agency (AFWA) dust emission module. In addition, we provide an example demonstration of output data from a simulation of a dust event that occurred in the Southwestern United States, which incorporates use of the drag partition.

15. SUBJECT TERMS
Aeolian processes, AFWA dust emission scheme, Computer simulation, Drag partition, Dust, Dust emission, Dust modeling, Dust storms, Friction speed, Vegetation, Visibility,WRF-Chem

16. SECURITY CLASSIFICATION OF:			17. LIMITATION OF ABSTRACT	18. NUMBER OF PAGES	19a. NAME OF RESPONSIBLE PERSON
a. REPORT	b. ABSTRACT	c. THIS PAGE			19b. TELEPHONE NUMBER (include area code)
Unclassified	Unclassified	Unclassified	SAR	47	